

SCIENTIFIC REPORTS



OPEN

In Vitro Micropatterned Human Pluripotent Stem Cell Test (μ P-hPST) for Morphometric-Based Teratogen Screening

Jiangwa Xing¹, Yue Cao^{1,2}, Yang Yu^{1,3,4}, Huan Li¹, Ziwei Song^{1,4} & Hanry Yu^{1,2,3,4,5}

Exposure to teratogenic chemicals during pregnancy may cause severe birth defects. Due to high inter-species variation of drug responses as well as financial and ethical burdens, despite the widely use of *in vivo* animal tests, it's crucial to develop highly predictive human pluripotent stem cell (hPSC)-based *in vitro* assays to identify potential teratogens. Previously we have shown that the morphological disruption of mesoendoderm patterns formed by geometrically-confined cell differentiation and migration using hPSCs could potentially serve as a sensitive morphological marker in teratogen detection. Here, a micropatterned human pluripotent stem cell test (μ P-hPST) assay was developed using 30 pharmaceutical compounds. A simplified morphometric readout was developed to quantify the mesoendoderm pattern changes and a two-step classification rule was generated to identify teratogens. The optimized μ P-hPST could classify the 30 compounds with 97% accuracy, 100% specificity and 93% sensitivity. Compared with metabolic biomarker-based hPSC assay by Stemina, the μ P-hPST could successfully identify misclassified drugs Bosentan, Diphenylhydantoin and Lovastatin, and show a higher accuracy and sensitivity. This scalable μ P-hPST may serve as either an independent assay or a complement assay for existing assays to reduce animal use, accelerate early discovery-phase drug screening and help general chemical screening of human teratogens.

The decreasing fertility rate and increasing age of pregnant women make healthy pregnancy a top priority for global health^{1,2}. Exposure to teratogenic compounds during pregnancy can disrupt normal embryo development and cause early embryo death, growth retardation, or severe birth defects. Currently most companies still rely on *in vivo* animal tests for predicting potential teratogens, which have been considered as the regulatory gold standard for decades³. However, due to large number of animals required and high inter-species variations in compound responses⁴, these costly and time-consuming animal tests are usually performed at a very late stage of compound development in at least two species and the general concordance to human responses is not very satisfactory⁵. Therefore, alternative *in vitro* human pluripotent stem cells (hPSCs)-based tests with reasonable accuracy should be developed and validated to establish regulatory standards⁶.

Currently available hPSC-based models, together with those animal cell-based models, mainly focus on recapitulating temporal disruptions of cell proliferation and/or differentiation by teratogenic compounds using various molecular biomarkers such as proteins^{7,8}, genes⁹, activity of specific signaling pathways¹⁰ or metabolites⁶. However, *in vivo* embryo development is a very complex process, which involves not only cell proliferation and differentiation, but also series of morphogenic movements spatially and temporally¹¹⁻¹³. Disruption of cell proliferation and/or differentiation may only partially identify teratogenic effects of test compounds. Previously we have developed the first *in vitro* human development model mimicking spatiotemporally controlled mesoendoderm development using micropatterning, where both cell differentiation and cell migration were modeled and

¹Institute of Bioengineering and Nanotechnology, A*STAR, The Nanos, #04-01, 31 Biopolis Way, Singapore, 138669, Singapore. ²Mechanobiology Institute, National University of Singapore, T-Lab, #05-01, 5A Engineering Drive 1, Singapore, 117411, Singapore. ³BioSyM, Singapore-MIT Alliance for Research and Technology, Enterprise Wing 04-13/14 and B1, 1 Create Way, Singapore, 138602, Singapore. ⁴Department of Physiology, Yong Loo Lin School of Medicine, MD9-04-11, 2 Medical Drive, Singapore, 117597, Singapore. ⁵Gastroenterology Department, Southern Medical University, Guangzhou, 510515, China. Correspondence and requests for materials should be addressed to J.X. (email: jwxing@ibn.a-star.edu.sg) or H.Y. (email: hanry_yu@nuhs.edu.sg)

quantified¹⁴. A confluent monolayer of circular hPSC colonies were patterned onto the tissue culture surface, and exposed to mesoendoderm induction medium for 3 days. Due to higher mechanical stress at the colony periphery compared with interior, cells at the periphery would differentiate into mesoendoderm cells¹⁵ and migrate inwards to form a consistent mesoendoderm pattern on day 3¹⁴. When dosing with paradigm teratogens, any disruptions on normal cell differentiation and collective cell migration could be captured by quantifying the morphology changes of the formed mesoendoderm patterns. A proof-of-concept testing using four known teratogens and one non-teratogen showed its improvement of teratogen detection compared to the mouse embryonic stem cell test (mEST).

In order to further develop this *in vitro* micropatterned hPSC (μ P-hPSC) model for industrial applications, here we optimized and validated the assay with a group of 30 compounds. We acquired the cytotoxicity profile of each compound on both human embryonic cell line H9 cells and adult human dermal fibroblasts (aHDFs), and tested the dose response of each compound in the μ P-hPSC colonies under mesoendoderm development. After acquiring the fluorescent images of mesoendoderm marker Brachyury (T) of the μ P-hPSC colonies, we identified the most sensitive morphological features to reflect the major compound-induced mesoendoderm pattern changes. The lowest disruption concentration (LDC) of each compound was identified based on the reduced features. We also developed a two-step classification rule for the teratogen identification to establish the *in vivo* relevance of the compound screening in our micropatterned human pluripotent stem cell test (μ P-hPST). This refined and validated assay with high predictability for teratogen detection would find wide applications in not only drug development but also as a cost-saving assay for early detection of teratogens in industrial chemicals, household and consumer goods, food and nutraceuticals, cosmetics and environmental toxins. This human cell-based *in vitro* assay will resolve the inter-species variation problems of the existing assays and contribute greatly to the reduction of animal uses.

Results

Cytotoxicity profile of test compounds. A set of 30 compounds of known teratogenicity was selected to establish and validate the μ P-hPST (Table 1). The compounds include equal number of non-teratogens and teratogens, and differ in chemical property and therapeutic usage. Before tested in the μ P-hPSC colonies, the cytotoxicity profile of each compound was acquired. Two cell lines, hPSC line H9 and adult human dermal fibroblast line aHDF, were tested to represent embryonic cytotoxicity and general cytotoxicity of the compound respectively (Supplementary Figs S1, S2). The IC_{25} values, which were the 25% inhibitory concentrations, were calculated as the highest non-cytotoxic concentrations of the compound (Table 2, Fig. 1). Generally, compounds which were toxic at very low concentrations were mostly teratogens, such as Doxorubicin, 5-Fluorouracil, Sunitinib and Lovastatin (IC_{25} values $< 1 \mu\text{g/ml}$); while compounds which showed minimum toxicity were mostly non-teratogens, such as Amoxicillin, Folic acid and Thiamine (IC_{25} values $> 800 \mu\text{g/ml}$) (Fig. 1). Similarity in cytotoxicity profile could be found in compounds belonging to the same class of chemical property or therapeutic use, especially in terms of general cytotoxicity. Antineoplastic drugs (5-Fluorouracil, Diethylstilbestrol, Doxorubicin and tyrosine kinase inhibitors (TKIs)) showed general cytotoxicity at relatively low concentrations ($IC_{25\text{aHDF}} < 10 \mu\text{g/ml}$) compared with other classes. Three of the four tested TKIs (Gefitinib, Imatinib and Sunitinib) exhibited higher general cytotoxicity than embryonic cytotoxicity, similar to antihypertensive compounds Methyldopa and Bosentan. Ethanolamine-based Histamine-1 antagonist Diphenhydramine and Doxylamine had similar general cytotoxicity ($IC_{25\text{aHDF}} = 31.4$ vs $45 \mu\text{g/ml}$), but varied greatly in terms of embryonic cytotoxicity ($IC_{25\text{H9}} = 2.4$ vs $87 \mu\text{g/ml}$). Loratadine, a piperidine Histamine H1 receptor antagonist, on the other hand, showed a much higher general cytotoxicity than Diphenhydramine and Doxylamine ($IC_{25\text{aHDF}} = 3.2 \mu\text{g/ml}$). While Vitamins Folic acid (Vitamin B9) and Thiamine (Vitamin B1) exhibited minimal toxicity to cells, Ascorbic acid (Vitamin C) showed toxicity at a much lower concentration and exhibited higher general cytotoxicity ($IC_{25\text{aHDF}} = 63 \mu\text{g/ml}$ $< IC_{25\text{H9}} = 105 \mu\text{g/ml}$). No obvious correlation was observed between compounds' teratogenicity potential and their higher embryonic cytotoxicity. There was similar number of compounds that had higher embryonic cytotoxicity than their general cytotoxicity in both non-teratogens and teratogens (5 VS 8, Fig. 1).

The cytotoxicity of compounds may interfere with their teratogenic effects and disrupt the mesoendoderm pattern formation in μ P-hPSC colonies. Therefore, the $IC_{25\text{aHDF}}$ and $IC_{25\text{H9}}$ values of each compound served as the cytotoxicity thresholds for teratogen testing and classification in our μ P-hPST.

Dose-dependent mesoendoderm pattern disruptions by test compounds. The key test of the μ P-hPST is to examine the morphological disruption effects of teratogenic compounds on μ P-hPSC colonies during mesoendoderm formation. In normal mesoendoderm induction medium without compound exposure, cells at the periphery of the μ P-hPSC colonies would always differentiate into T^+ mesoendoderm cells and migrate inwards to form a consistent annular mesoendoderm pattern after 3 days of culture¹⁴. Teratogen would affect the cell differentiation and/or migration process and change the morphology of the mesoendoderm patterns in a dose-dependent manner. To explore the teratogenic potential of test compounds, we selected 6 concentrations of each compound and tested them on the μ P-hPSC colonies. The concentrations were selected to cover compound's cytotoxicity thresholds ($IC_{25\text{aHDF}}$ and $IC_{25\text{H9}}$) as well as its highest therapeutic concentration in human plasma (C_{max}) (Table 2, Supplementary Table. S1). The μ P-hPSC colonies were incubated in mesoendoderm induction medium together with the test compounds for 3 days. The medium was half changed every day. On day 3, all the colonies were fixed and immunostained for mesoendoderm marker T, the distribution of which indicated the morphology of the mesoendoderm patterns (Supplementary Fig. S3).

From the T fluorescent images, we could see that most non-teratogens showed no obvious disruption effects compared with teratogens even at the highest dose except Acyclovir, Ascorbic acid, Diphenhydramine, Metoclopramide and Thiamine (Fig. 2b, Supplementary Fig. S3a,b). Most teratogens, on the contrary, were observed with a clear dose-dependent response within the test range (Fig. 2b, Supplementary Fig. S3c,d). Different

| Drug name | Chemical property | Therapeutic use | FDA label | In vivo teratogenicity |
|--------------------|---|---|-----------|------------------------|
| Acetaminophen | Derivative of acetanilide | Analgesic and antipyretic | B | NON |
| Acyclovir | Nucleoside analog, DNA polymerase Inhibitor. | Antiviral, to treat herpes labialis and genital herpes | B | NON |
| Amoxicillin | Penicillin | Antibiotic | B | NON |
| Ascorbic acid | Vitamin C | To treat or prevent vitamin C deficiency | A | NON |
| Caffeine | Methylxanthine, adenosine receptor antagonist, phosphodiesterase inhibitor | Central nervous system stimulant, anti-inflammatory | C | NON |
| Diphenhydramine | Ethanolamine-based Histamine-1 antihistamine | Antiemetic, antitussive, anti-allergic, hypnotic and sedative | B | NON |
| Doxylamine | Ethanolamine-based Histamine-1 antihistamine | To treat allergy symptoms and insomnia; also used as an antitussive and antiemetic | A | NON |
| Esomeprazole | Proton pump inhibitor | Anti-ulcer, gastric acid secretion inhibitor and gastrointestinal agent | B | NON |
| Folic acid | Vitamin B9 | To treat or prevent folate deficiencies and megaloblastic anemia | A | NON |
| Isoniazid | Synthetic derivative of nicotinic acid | Antitubercular | C | NON |
| Loratadine | Piperidine Histamine H1 receptor antagonist | Antipruritic and anti-allergic, to treat allergic rhinitis and urticaria | B | NON |
| Metoclopramide | Dopamine D2 antagonist | Gastroprokinetic and antiemetic | B | NON |
| Methyldopa | Adrenergic alpha2-Agonist | Antihypertensive | B | NON |
| Sitagliptin | Dipeptidyl peptidase 4 inhibitor | Hypoglycemic, to treat type 2 diabetes | B | NON |
| Thiamine | Vitamin B1 | To treat or prevent vitamin B1 deficiency | A | NON |
| 5-Fluorouracil | Nucleoside metabolic inhibitor | Antineoplastic | D | TER |
| Bosentan | Endothelin receptor antagonist | Antihypertensive, to treat pulmonary artery hypertension | X | TER |
| Busulfan | Alkylating agent | Anti-Leukemia | D | TER |
| Carbamazepine | Tricyclic compound chemically related to tricyclic antidepressants (TCA) | Anticonvulsant and analgesic | D | TER |
| Diethylstilbestrol | Non-steroidal oestrogen hormone | Antineoplastic, to treat breast and prostate cancer | X | TER |
| Diphenylhydantoin | Hydantoin derivative | Anticonvulsant | D | TER |
| Doxorubicin | Anthracycline topoisomerase inhibitor | Antineoplastic | D | TER |
| Furosemide | Sulfamoylanthranilic acid derivative | Diuretic; to treat hypertension and edema | C | TER |
| Gefitinib | Tyrosine kinase inhibitor, EGFR inhibitor | Antineoplastic, to treat lung cancer | D | TER |
| Imatinib | Tyrosine kinase inhibitor, inhibiting Bcr-Abl fusion protein tyrosine kinase, PDGFR and SCF/c-kit | Anti-Leukemia and antineoplastic, to treat dermatofibrosarcoma protuberans and malignant gastrointestinal stromal tumors | D | TER |
| Lovastatin | HMG-CoA reductase inhibitor | Anticholesteremic | X | TER |
| Methimazole | Thyroid hormone synthesis inhibitor | Antithyroid, to treat hyperthyroidism | D | TER |
| Sunitinib | Tyrosine kinase inhibitor, inhibiting VEGFR2, PDGFRb, c-kit, and FLT3 | Antineoplastic, to treat gastrointestinal stromal tumor, pancreatic neuroendocrine tumor, and advanced renal cell carcinoma | D | TER |
| Vandetanib | Tyrosine kinase inhibitor, inhibiting VEGFR2 and EGFR | Antineoplastic, to treat symptomatic or progressive medullary thyroid cancer | D | TER |
| Ziprasidone | Benzothiazolylpiperazine derivative; antagonist at the dopamine D2, serotonin 5-HT2A, 5-HT1A, 5-HT1D receptors; | Antipsychotic, to treat Bipolar I disorder and Schizophrenia | C | TER |

Table 1. Description of test compounds. The chemical properties and usages of drugs were found in PubChem Open Chemistry Database (<https://pubchem.ncbi.nlm.nih.gov>). NON: Non-teratogen, TER: Teratogen.

disruption patterns could be identified from the images. The compounds could slow down or prevent mesoendoderm cell migration, for instance, in the case of Thiamine and Diphenylhydantoin; or promote cell migration, as in the case of Diethylstilbestrol and Lovastatin. They could also decrease both cell differentiation and migration, as in the case of Carbamazepine; or promote both cell differentiation and migration, as in 5-Fluorouracil; or even promote mesoendoderm differentiation while decrease collective cell migration, as in Methimazole and Sunitinib. Beside teratogenicity, cytotoxicity effects could also affect mesoendoderm patterns. For example, under Busulfan treatment at concentrations higher than 0.5 $\mu\text{g}/\text{ml}$, which is its $\text{IC}_{25\text{H}9}$ value, cell number in the μP -hPSC colonies decreased. Together with the compound's migration acceleration effects, much smaller and concentrated mesoendoderm patterns were observed (Supplementary Fig. S3c). At concentration of 10 $\mu\text{g}/\text{ml}$, only a thin monolayer of cells remained within the colony and the mesoendoderm pattern was totally lost.

Morphological feature selection to capture compounds' disruption effects. Since various morphological disruption patterns were acquired after compound treatment, a quantitative, multi-variate image characterization method was needed to measure the disruption effects and identify the lowest disruption

| Drug name | IC _{25aHDF} (µg/ml) | IC _{25H9} (µg/ml) | C _{max} (µg/ml) | LDC (µg/ml) | Step1: Is LDC ≤ IC _{25aHDF} & IC _{25H9} ? | Step 2: Is LDC ≤ 10 C _{max} ? | Teratogenicity in µP-hPST | Teratogenicity in other <i>in vitro</i> assays | <i>In vivo</i> teratogenicity |
|--------------------|------------------------------|----------------------------|--------------------------|-------------|---|--|---------------------------|--|-------------------------------|
| Acetaminophen | 40 | 171 | 24 | 160 | N | - | NON | NON ⁶ | NON |
| Acyclovir | 285 | 267 | 5.65 | 60 | Y | N | NON | NON ^{6,7} | NON |
| Amoxicillin | >1000 | >1000 | 14.4 | 150 | Y | N | NON | NON ⁶ | NON |
| Ascorbic acid | 63 | 105 | 156 | 80 | N | — | NON | NON ⁶ | NON |
| Caffeine | 129 | 85.4 | 10 | 130 | N | — | NON | NON ^{6,7} | NON |
| Diphenhydramine | 31.4 | 2.4 | 0.06 | 2.4 | Y | N | NON | NON ⁶ | NON |
| Doxylamine | 45 | 87 | 0.12 | 45 | Y | N | NON | NON ⁶ | NON |
| Esomeprazole | 42.1 | 38.9 | 1.62 | 45 | N | — | NON | NON ⁷ | NON |
| Folic acid | 894 | 888 | 0.27 | 900 | N | — | NON | NON ⁶ | NON |
| Isoniazid | 488 | 370 | 3.09 | 500 | N | — | NON | NON ⁶ | NON |
| Loratadine | 3.2 | 24 | 0.04 | 4 | N | — | NON | NON ⁶ | NON |
| Metoclopramide | 154 | 162 | 0.04 | 120 | Y | N | NON | NON ⁶ | NON |
| Methyldopa | 15.9 | 23.2 | 7.5 | 25 | N | — | NON | NON ⁷ | NON |
| Sitagliptin | 77.1 | 359 | 0.39 | >360 | N | — | NON | NON ⁶ | NON |
| Thiamine | >1000 | >1000 | 0.11 | 1000 | Y | N | NON | NON ⁶ | NON |
| 5-Fluorouracil | 0.16 | 0.15 | 48.4 | 0.025 | Y | Y | TER | TER ^{6,7} | TER |
| Bosentan | 19.9 | 43.8 | 8.17 | 16 | Y | Y | TER | NON ⁶ | TER |
| Busulfan | 19.2 | 0.5 | 1.22 | 0.2 | Y | Y | TER | TER ⁶ | TER |
| Carbamazepine | 28 | 21 | 11 | 10 | Y | Y | TER | TER ⁶ | TER |
| Diethylstilbestrol | 6.1 | 8.8 | 0.0056 | 5 | Y | N | NON | TER ⁷ | TER |
| Diphenylhydantoin | 140 | 56 | 20 | 50 | Y | Y | TER | NON ⁶ | TER |
| Doxorubicin | 0.003 | 0.0002 | 0.37 | 0.00015 | Y | Y | TER | TER ⁷ | TER |
| Furosemide | 30 | 362 | 400 | 30 | Y | Y | TER | NON ²⁸ | TER |
| Gefitinib | 1.66 | 4.6 | 0.93 | 0.9 | Y | Y | TER | TER ⁷ | TER |
| Imatinib | 2.7 | 19.5 | 1.56 | 0.75 | Y | Y | TER | TER ⁷ | TER |
| Lovastatin | 0.68 | 0.30 | 0.01 | 0.01 | Y | Y | TER | NON ⁶ | TER |
| Methimazole | >1000 | 252 | 0.3 | 1.5 | Y | Y | TER | NA | TER |
| Sunitinib | 0.18 | 0.89 | 0.03 | 0.15 | Y | Y | TER | TER ⁷ | TER |
| Vandetanib | 1.1 | 0.3 | 0.4 | 0.3 | Y | Y | TER | TER ⁷ | TER |
| Ziprasidone | 2.7 | 14.4 | 0.2 | 1.25 | Y | Y | TER | TER ⁷ | TER |

Table 2. Compound screening results in µP-hPST. The C_{max} values of each compound were mainly acquired from U.S. Food and Drug Administration website, European Medicines Agency website or published journals unless otherwise noted. The full list could be found in Supplementary Table S1. NON: Non-teratogen, TER: Teratogen, NA: not applicable.

concentration (LDC) of each compound. Initially we extracted 19 morphological features from each T fluorescent image to characterize the spatial distribution of the mesoendoderm cells. They were the typical statistical data descriptors such as sum (area), mean (position), variance, kurtosis, etc. Four features were related to skewness and entropy that did not correlate with compound treatment¹⁴. Among the remaining 15 features, we clustered them into 7 morphological groups to quantify various compound disruptions. Plotting these compound disruption effects into box plots, we found that the high order statistical descriptors such as kurtosis and energy are less sensitive than the low order ones such as area, position, standard deviation (SD) and coefficient of variation (CV), in correlating with the compound-induced morphological changes at low concentrations. Therefore, only these four best morphological features were selected to quantitatively characterize the mesoendoderm patterns among groups (Fig. 2a).

To identify the LDC of a test compound, we plotted the values of these four features from all dose groups and compared with the untreated controls respectively using unpaired two sample t-tests (Fig. 2c, Supplementary Fig. S4). A significant disruption was defined as $p < 0.01$. The lowest concentration which showed a significant morphological disruption without a breaking point at higher concentrations in at least one of the four features would be defined as the LDC (Fig. 2c, Supplementary Fig. S4).

Generation of a two-step teratogen classification method. After the LDC values of all test compounds were identified in µP-hPST (Table 2), compound classification was performed. Since the cytotoxicity of compounds may also disrupt the mesoendoderm pattern formation, we first compared the LDC values with the IC₂₅ values of aHDF and H9 cells. The LDC of teratogens should be no higher than their IC_{25aHDF} and IC_{25H9} values. Otherwise, the test compound could be classified as a non-teratogen. By using this rule, 9 of the 30 compounds would be classified as non-teratogens and the remaining 21 compounds would be classified as teratogens (Table 2). All of the 9 non-teratogens were consistent with their *in vivo* classifications; however, 6 of the identified

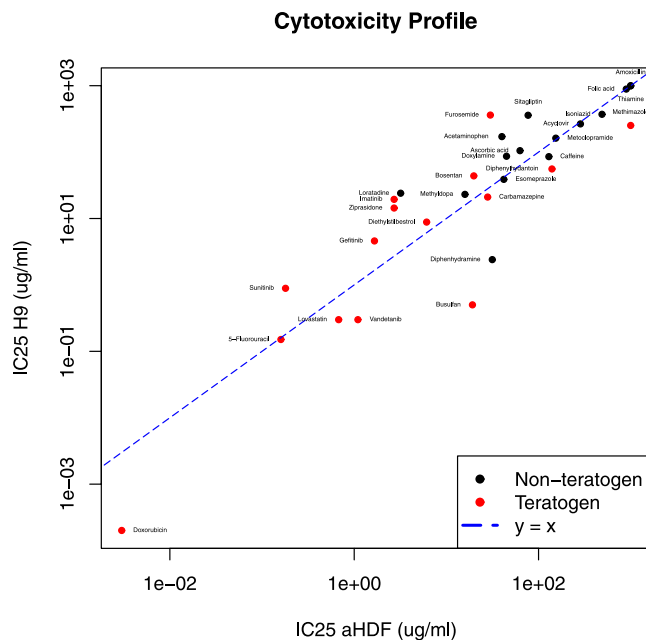


Figure 1. Cytotoxicity profile of test compounds Red: teratogens, Black: non-teratogens.

teratogens were misclassified. When comparing their LDC values with their respective C_{max} values, we found that the LDC values were much higher, indicating that the physiological relevance should also be taken into account. To achieve this, a second step of the classification was implemented to examine the *in vivo* relevance (Fig. 3). A threshold using a scale factor of C_{max} was applied. If the LDC of a test compound were higher than the scale factor of C_{max} , which means this teratogenic effect was unlikely to happen clinically, we would classify the compound as a non-teratogen; otherwise, it be a teratogen (Fig. 3).

To investigate the value of scale factor for C_{max} , we had all 21 unclassified compounds tested using leave-one-out rule after Step 1^{16,17}. The LDC and C_{max} values of the compounds, together with their known teratogenicity class served as inputs to the model to find the optimal scale factor (Supplementary Table S2). Results showed that a scale factor of 7–10 could achieve the best classification accuracy across all test runs (AUC \geq 96%) (Supplementary Fig. S4), with only Diethylstilbestrol misclassified as false positive (Fig. 4, Table 2). To verify such optimal scale factor, we also had LDC and C_{max} used as features and thus created a binary classification model using multinomial logistic regression (MLR) and support vector machine (SVM). The binary classification results (AUC = 91.7% for both MLR and SVM) were comparable to the scale factor based classification with only one compound being misclassified (Supplementary Fig. S6) and thus proved that second step of proposed classification rule could recapitulate the inherent difference of the tested compounds.

Assay performance. By extracting four morphological features to find LDC and a two-step classification method to classify the compounds, we could improve our μ P-hPST assay to achieve 97% accuracy, 100% specificity and 93% sensitivity in screening 30 paradigm compounds (Table 3). We compared our assay performance with the Targeted Biomarker Assay⁶, which is one of the state-of-the-art hPSC-based teratogen screening models. The assay measures the ratio of two metabolites which are Ornithine and Cystine in hPSC maintenance culture to identify compound's disruption concentration, and compares it with *in vivo* C_{max} to classify the compound's teratogenicity⁶. The μ P-hPST captures the disruption of mesoendoderm patterns by affecting spatiotemporally controlled cell differentiation and migration, and exhibits better performance in terms of accuracy, sensitivity and specificity. It could correctly classify Bosentan, Diphenylhydantoin and Lovastatin, which were all misclassified in the Targeted Biomarker Assay (Table 3). It can also correctly identify Furosemide as teratogen which was misclassified in MEST (Table 2).

Discussion

Precise control of cell differentiation and migration patterns is critical during all stages of the embryo development^{18–21}. Teratogens could disrupt embryo development through interfering cell differentiation and morphogenetic movements, resulting in various birth defects. Currently one of the most accurate and commonly used clinical examinations for teratogenicity is direct morphological observations using B-mode ultrasonography. For *in vitro* teratogen screenings, some studies have examined the morphological changes due to teratogenic disruptions in both cell differentiation and migration using animal embryos or cells, such as the rat whole embryo culture (rWEC) assay²², the zebrafish embryo culture (ZEC) assay^{23,24}, and a newly developed assay using mouse embryoid body (mEB) by Marikawa's group^{25,26}. However, these assays are under performing (~70–80% accuracy for the rWEC and ZEC assays)²⁷. We have established the first *in vitro* hPSC-based and fully quantitative morphometric assay which captured both cell differentiation and cell migration processes, and successfully eliminated inter-species variations¹⁴. Refined and validated using 30 compounds, our μ P-hPST exhibited the highest accuracy compared with other existing *in vitro* teratogen screening models using animal embryos and cells^{8,10,22,24,27,28}, or hPSCs^{6,7}.

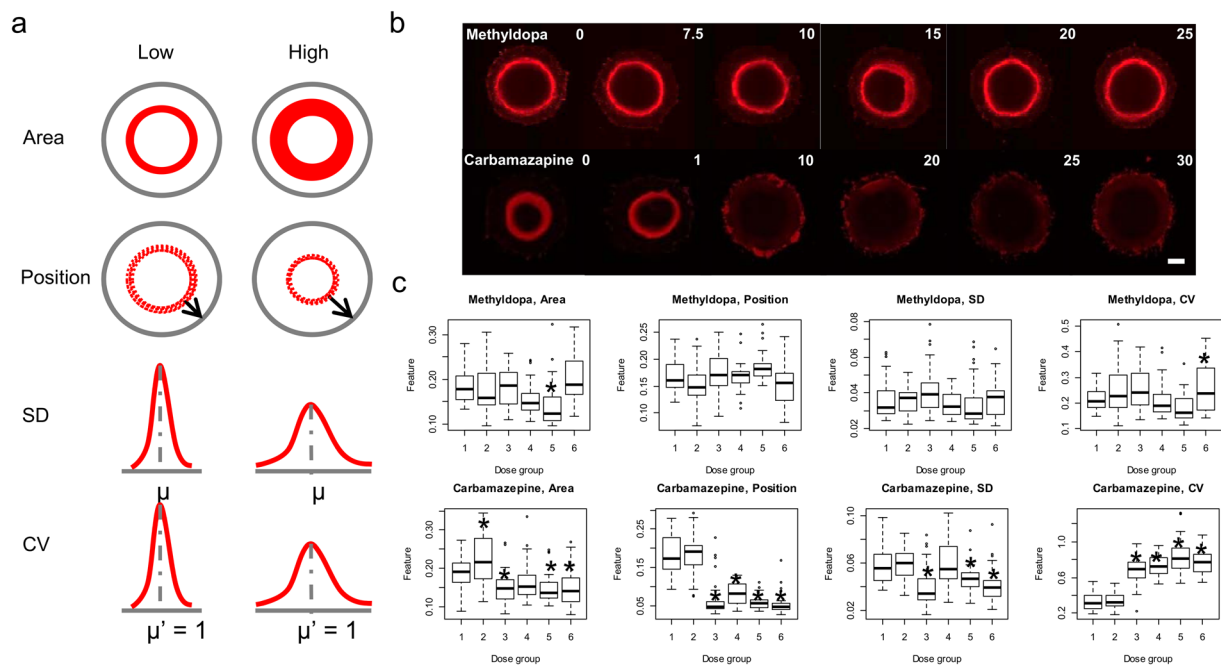


Figure 2. Morphological features showing the dose-dependent response of mesoendoderm pattern disruption. (a) The four features extracted from T fluorescent images. SD: Standard deviation; CV: Coefficient of variation. μ , μ' : Mean. (b) Representative T fluorescent images after drug treatment. Methyldopa: non-teratogen; Carbamazepine: teratogen. Scale bar, 200 μm . (c) Boxplots of the morphological features after Methyldopa and Carbamazepine treatment. Dose groups (1–6): 0, 7.5, 10, 15, 20, 25 $\mu\text{g}/\text{ml}$ for Methyldopa, 0, 1, 10, 20, 25, 30 $\mu\text{g}/\text{ml}$ for Carbamazepine. * $p < 0.01$. The LDC for Methyldopa and Carbamazepine are 25 $\mu\text{g}/\text{ml}$ and 10 $\mu\text{g}/\text{ml}$ respectively.

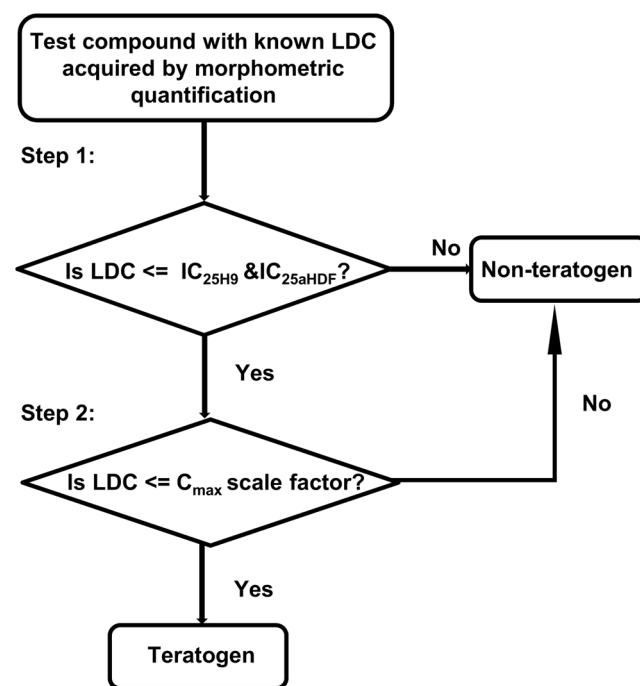


Figure 3. Two-step decision rule for teratogen classification.

The $\mu\text{P-hPST}$ recapitulated the mesoendoderm formation process which occurs during gastrulation. One key reason is that the spatial and temporal control of primitive streak formation and mesoendoderm generation is critical in initiating the correct human body plan, which is followed by the three germ layer generation and organogenesis^{29,30}. By quantifying the morphological disruptions of the cell differentiation and collective cell

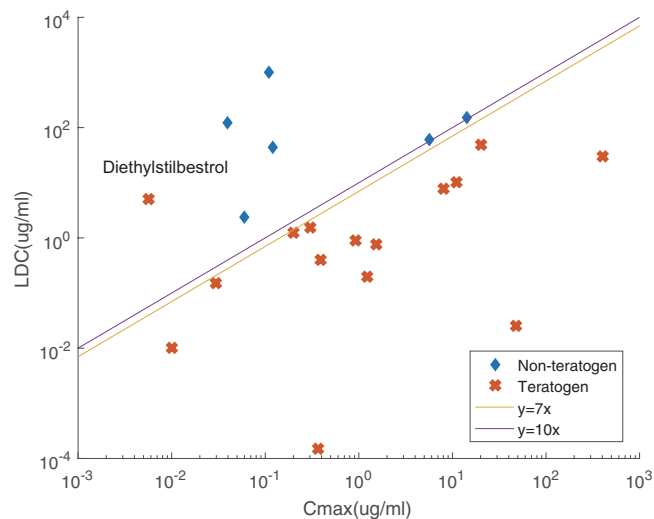


Figure 4. Linear comparison results for the identification of best C_{max} scale factor. Only Diethylstilbestrol was misclassified as a non-teratogen when Step 2 of the classification rule was $LDC \leq 7\text{--}10$ fold of C_{max} for teratogens.

| Assay | No. of compounds | Sensitivity | Specificity | Accuracy |
|--------------------------|------------------|-------------|-------------|----------|
| μ P-hPST | 30 | 93% | 100% | 97% |
| Targeted Biomarker Assay | 36 | 79% | 100% | 89% |

Table 3. Summary of the μ P-hPST assay performance.

migration patterns that are the two critical processes in every stage of the embryonic development, we could detect teratogens affecting not just mesoendoderm but also the other stages of embryo development. For example, the μ P-hPST can detect the teratogenic effects of Diphenylhydantoin and Carbamazepine. Diphenylhydantoin is known to induce orofacial, limb, cardiovascular and neurobehavioral anomalies^{6,31}, and Carbamazepine could cause neural tube defects, cardiovascular and urinary tract anomalies, and cleft palate in newborns³².

Dose-dependent response is a key feature of compounds' teratogenic effects. The identification of human teratogens always correlates with their clinical therapeutic dose. Therefore, it's crucial to compare the *in vitro* teratogenic concentration range with their *in vivo* therapeutic dose when screening teratogens *in vitro*. In this study, without comparing the *in vitro* LDC with the *in vivo* C_{max} of the test compounds, the assay would yield high false positive rate ($6/21 = 28.6\%$). The second step of the classification approach was established based on an intuitive linear relationship assumption between LDC and C_{max} , and verified using MLR and SVM binary classification models with comparable classification accuracy. After applying a second classification step which excluded compounds whose LDC was higher than 7–10 fold of C_{max} , only one false negative result was observed. This two-step classification rule was also applicable to the five paradigm compounds tested previously¹⁴, all the compounds (one known non-teratogen and four teratogens) could still be correctly classified (Supplementary Table S3). For predictability of teratogen identification among unknown compounds, the two-step classification method has its unique advantages compared with the Targeted Biomarker Assay, which uses C_{max} as a reference for classification⁶. For compounds with unknown C_{max} , the μ P-hPST can quickly identify candidates which are more likely non-teratogens by acquiring all negatives in Step 1 of the classification rule, and provide useful information regarding the potential *in vivo* teratogenic concentration range for those with uncertain teratogenicity.

The μ P-hPST achieved 97% accuracy using the two-step classification method in the current teratogen screen of 30 compounds, among which the identified teratogens could affect different stages of embryonic development with different mechanisms of teratogenicity. However, considering the complexity of the teratogenic mechanisms, more teratogen screens using additional compounds are required to further test the predictability of our current assay. These compounds may include chemicals of different chemical classes and usages, or compounds which have differential teratogenic effects but share similar chemical structures.

Although *in vivo* animal assays have been used for teratogen screening for decades and are required by regulatory bodies, they cannot fully reproduce human responses due to high inter-species variations ($\sim 40\%$)⁵. False negatives generated by these *in vivo* animal models due to species variability have caused irreversible social tragedies such as the case of Thalidomide³³. An increase from testing one animal species to two could lower the chance of false negatives to $\sim 12.5\%$ (by keeping the 40% species variability consistent), but would significantly increase the false positive rate⁵. Our μ P-hPST is an *in vitro* hPSC-based assay which eliminates the inter-species variability, and has much better prediction accuracy (97% accuracy, 100% specificity and 93% sensitivity) compared with both *in vivo* animal models and other existing *in vitro* assays. However, it still cannot detect all teratogenic

compounds possibly due to the inherent limitations shared by all *in vitro* assays (1 in 15 teratogens was classified as false negative). A combination of the μ P-hPST with a second *in vivo* or *in vitro* assay may serve as an option for human teratogen detection. For compounds with existing animal testing data, the use of μ P-hPST could eliminate potential false negatives by providing human-specific testing results. As for new compounds screening, the μ P-hPST could be first applied to save costs and time, and comparing the negatives with further *in vivo* animal test. The μ P-hPST could best serve as an early-phase teratogen screening assay for pharmaceutical companies and research institutions, or a late phase verification of animal testing results.

Conclusion

The μ P-hPST is the first *in vitro* hPSC-based morphometric assay for human teratogen screening, which could capture compound's teratogenic effects in both cell differentiation and collective cell migration. It eliminated inter-species variations, and achieved 100% specificity, 93% sensitivity and 97% accuracy in 30 compound screen. The μ P-hPST could serve as a good teratogen-screening assay independently or complementing other assays to reduce animal use, accelerate early discovery-phase drug screening, or general chemical screening.

Materials and Methods

Compounds. All compounds used in this study were purchased from Selleck Chemicals or Sigma-Aldrich: 5-Fluorouracil (F6627, Sigma-Aldrich), Acetaminophen (A7085, Sigma-Aldrich), Acyclovir (S1807, Selleck Chemicals), Amoxicillin (S3015, Selleck Chemicals), Ascorbic acid (A5960, Sigma-Aldrich), Bosentan (S4220, Selleck Chemicals), Busulfan (B2635, Sigma-Aldrich), Caffeine (27600, Sigma-Aldrich), Carbamazepine (C8981, Sigma-Aldrich), Diethylstilbestrol (D4528, Sigma-Aldrich), Diphenhydramine (S1866, Selleck Chemicals), Diphenylhydantoin (D4007, Sigma-Aldrich), Doxorubicin (S1208, Selleck Chemicals), Doxylamine (D3775, Sigma-Aldrich), Esomeprazole (S1743, Selleck Chemicals), Folic acid (F7876, Sigma-Aldrich), Furosemide (F4381, Sigma-Aldrich), Gefitinib (S1025, Selleck Chemicals), Imatinib (S1026, Selleck Chemicals), Isoniazid (S1937, Selleck Chemicals), Loratadine (S1358, Selleck Chemicals), Lovastatin (S2061, Selleck Chemicals), Methimazole (S1609, Selleck Chemicals), Methyl dopa (S1642, Selleck Chemicals), Metoclopramide (M0763, Sigma-Aldrich), Sitagliptin (S4002, Selleck Chemicals), Sunitinib (S1042, Selleck Chemicals), Vandetanib (S1046, Selleck Chemicals), Thiamine (T4625, Sigma-Aldrich), Ziprasidone (S1444, Selleck Chemicals).

All compounds were dissolved in DMSO (D2650, Sigma-Aldrich) except the following compounds, which were dissolved in culture medium: Acyclovir, Caffeine, Methimazole, Isoniazid, Folic acid and Thiamine.

Cell maintenance and differentiation. Human embryonic cell line H9 (WiCell Research Institute, Inc) and adult human dermal fibroblast (aHDF, Lonza) were cultured as previously described¹⁴. Briefly, H9 cells were cultured in tissue culture plates coated with Matrigel™ (354277, BD Biosciences) in mTeSR™1 medium (05850, StemCell™ Technologies). Dispase (07923, StemCell™ Technologies) treatment and mechanical scraping were applied during normal subculture. The aHDF cells were cultured in DMEM medium (10569-010, Gibco), supplemented with 10% FBS (SV30160.03, Thermo Scientific Hyclone) and 1% Pen-Strep (09367-34, Nacalai Tesque). Cells were subcultured every 5–6 days using 0.25% Trypsin-EDTA (25200-114, Gibco) to detach the cells.

To induce mesoendodermal differentiation, H9 cells were cultured in serum-free STEMdiff™ APEL™ medium (05210, StemCell™ Technologies) supplemented with 100 ng/ml Activin A (338-AC-025, R&D Systems), 25 ng/ml BMP4 (314-BP-010, R&D Systems) and 10 ng/ml FGF2 (233-FB-025, R&D Systems). For compound testing in the μ P-hPST, the final concentration of DMSO in the medium was lower than 0.5%.

Cytotoxicity assay. The adverse effect of test compounds on cell proliferation and viability was detected using CellTiter 96® Aqueous One Solution Cell Proliferation Assay (MTS, G3580, Promega). 10,000 H9 cells or 500 aHDF cells were seeded in 96-well tissue culture plates. For H9 cells, Matrigel™ was coated before seeding. For each compound, 8 concentrations from serial 5-fold dilutions were tested besides the vehicle controls. Cells were cultured for 3 days with medium half change every day before cell viability was measured. Each drug was tested in three independent runs and its IC₂₅ values (inhibitory concentrations which can cause 25% of reduction in cell number) were acquired by logistic regression using OriginPro 9.

Generation of μ P-hPSC colonies. The polydimethylsiloxane (PDMS) stencil was fabricated as previously described¹⁴. Circular patterns with 1 mm in diameter were generated on each stencil, which is in square shape and fit for 60-mm dishes. To generate μ P-hPSC colonies, autoclaved PDMS stencils were sealed onto tissue culture dishes using 70% ethanol, and coated with 300 μ l Matrigel™ diluted in DMEM/F12 (11330032, GIBCO) for 5 hr at 37 °C. For cell seeding, single cells were acquired using Accutase (SCR005, Merck Millipore), and seeded at 5190 cells/mm² in cell maintenance medium containing 10 μ M Y27632 (688000, Calbiochem, Merck Millipore). After 45 min, stencils were peeled off and the surface was treated with 0.5% Pluronic F-127 (P2443, Sigma-Aldrich) in DMEM/F12 for passivation. Cells were incubated for at least 3 hr in Y27632-containing medium before switched to normal mTeSR™1 medium. Differentiation started the next day.

Immunofluorescence staining and microscopy. On day 3 of differentiation, cells were fixed using 4% paraformaldehyde for immunofluorescence staining of mesoendoderm marker Brachyury (T). Cells were permeabilized with 0.5% Triton X-100 in 1X PBS and incubated in 2% BSA in 0.1% PBS Triton X-100 for 3 hr at room temperature (RT). Cells were incubated overnight with goat anti-Brachyury (AF2085, R&D Systems) primary antibody (1:100) at 4 °C and then incubated in Alexa Fluor® 546 donkey anti-goat IgG (A11056, Life Technologies) secondary antibody (1:1000) for 1 hr at RT after washing. Fluorescence imaging was done using Olympus IX81 epifluorescence microscope (Olympus, Japan).

Morphological feature extraction. Image analysis was performed using Matlab Image Processing Toolbox and Statistical Toolbox (Mathworks). The μ P-hPSC colonies were identified using intensity differences from background. Segmentation using Otsu's method was performed to identify T⁺ regions of the colonies. Four morphologic features including Area, Position, Standard deviation (SD) and Coefficient of variation (CV) of the T⁺ region were calculated to represent the morphological distribution of the mesoendoderm patterns.

Classification model. All the classification analysis was done using Matlab Statistical Toolbox (Mathworks). To identify the best scale factor of C_{max} for drug classification, linear comparison was performed using LDC and C_{max} values. The leave-one-out cross validation rule was applied. For each run, a factor ranging from 1 to 20 was tested with an interval of 1. Best parameters were then chosen based on the highest area under the receiver operating characteristic curve (AUC) values acquired in respective Receiver Operating Curve (ROC) evaluation. Multinomial logistic regression (MLR) and support vector machine (SVM) using leave-one-out cross validation approach were further utilized to verify the classification accuracy of linear comparison using LDC and C_{max} as input features. The performances were evaluated using their respective AUC values.

Statistical analysis. The statistical analysis was done in R (Version 3.1.2). Unpaired two-sample t-test was performed to evaluate statistical differences between compound-treated groups and control group. Differences were deemed as significant if $p < 0.01$. The first dose showing significant disruptions without breakpoint in the following higher concentrations will be determined as the LDC of test compound.

References

- Kancherla, V., Oakley, G. P. Jr. & Brent, R. L. Urgent global opportunities to prevent birth defects. *Semin Fetal Neonatal Med* **19**, 153–60 (2014).
- Hamilton, B. E., Martin, J. A. & Osterman, M. J. Births: preliminary data for 2015. *Natl Vital Stat Rep* **65**, 1–15 (2016).
- Daston, G. P. Laboratory models and their role in assessing teratogenesis. *Am J Med Genet C Semin Med Genet* **157C**, 183–7 (2011).
- Olson, H. *et al.* Concordance of the toxicity of pharmaceuticals in humans and in animals. *Regul Toxicol Pharmacol* **32**, 56–67 (2000).
- Bremer, S., Pellizzer, C., Hoffmann, S., Seidle, T. & Hartung, T. The development of new concepts for assessing reproductive toxicity applicable to large scale toxicological programmes. *Curr Pharm Des* **13**, 3047–58 (2007).
- Palmer, J. A. *et al.* Establishment and assessment of a new human embryonic stem cell-based biomarker assay for developmental toxicity screening. *Birth Defects Res B Dev Reprod Toxicol* **98**, 343–63 (2013).
- Kameoka, S., Babiarz, J., Kolaja, K. & Chiao, E. A high-throughput screen for teratogens using human pluripotent stem cells. *Toxicol Sci* **137**, 76–90 (2014).
- Seiler, A. E. & Spielmann, H. The validated embryonic stem cell test to predict embryotoxicity *in vitro*. *Nat Protoc* **6**, 961–78 (2011).
- Panzica-Kelly, J. M. *et al.* Establishment of a molecular embryonic stem cell developmental toxicity assay. *Toxicol Sci* **131**, 447–57 (2013).
- Uibel, F. & Schwarz, M. Prediction of embryotoxic potential using the ReProGlo stem cell-based Wnt reporter assay. *Reprod Toxicol* **55**, 30–49 (2015).
- Kimmel, C. B., Ballard, W. W., Kimmel, S. R., Ullmann, B. & Schilling, T. F. Stages of embryonic development of the zebrafish. *Dev Dyn* **203**, 253–310 (1995).
- Hogan, B. L. Morphogenesis. *Cell* **96**, 225–33 (1999).
- Lecuit, T. & Lenne, P.-F. Cell surface mechanics and the control of cell shape, tissue patterns and morphogenesis. *Nat. Rev. Mol. Cell Biol.* **8**, 633–644 (2007).
- Xing, J., Toh, Y. C., Xu, S. & Yu, H. A method for human teratogen detection by geometrically confined cell differentiation and migration. *Sci Rep* **5**, 10038 (2015).
- Toh, Y. C., Xing, J. & Yu, H. Modulation of integrin and E-cadherin-mediated adhesions to spatially control heterogeneity in human pluripotent stem cell differentiation. *Biomaterials* **50**, 87–97 (2015).
- Mikshowsky, A. A., Gianola, D. & Weigel, K. A. Assessing genomic prediction accuracy for Holstein sires using bootstrap aggregation sampling and leave-one-out cross validation. *J Dairy Sci* **100**, 453–464 (2017).
- Shao, Z., Er, M. J. & Wang, N. An efficient leave-one-out cross-validation-based extreme learning machine (ELOO-ELM) with minimal user intervention. *IEEE Trans Cybern* **46**, 1939–51 (2016).
- Noctor, S. C., Martinez-Cerdeno, V., Ivic, L. & Kriegstein, A. R. Cortical neurons arise in symmetric and asymmetric division zones and migrate through specific phases. *Nat Neurosci* **7**, 136–44 (2004).
- Thiery, J. P., Acloque, H., Huang, R. Y. & Nieto, M. A. Epithelial-mesenchymal transitions in development and disease. *Cell* **139**, 871–90 (2009).
- Shelton, E. L. & Yutzey, K. E. Twist1 function in endocardial cushion cell proliferation, migration, and differentiation during heart valve development. *Dev Biol* **317**, 282–95 (2008).
- Costantini, F. & Kopan, R. Patterning a complex organ: branching morphogenesis and nephron segmentation in kidney development. *Dev Cell* **18**, 698–712 (2010).
- Zhang, C. *et al.* Development of a streamlined rat whole embryo culture assay for classifying teratogenic potential of pharmaceutical compounds. *Toxicol Sci* **127**, 535–46 (2012).
- Gustafson, A. L. *et al.* Inter-laboratory assessment of a harmonized zebrafish developmental toxicology assay - progress report on phase I. *Reprod Toxicol* **33**, 155–64 (2012).
- Panzica-Kelly, J. M., Zhang, C. X. & Augustine-Rauch, K. A. Optimization and performance assessment of the chorion-off [dechorinated] zebrafish developmental toxicity assay. *Toxicol Sci* **146**, 127–34 (2015).
- Warkus, E. L., Yuen, A. A., Lau, C. G. & Marikawa, Y. Use of *in vitro* morphogenesis of mouse embryoid bodies to assess developmental toxicity of therapeutic drugs contraindicated in pregnancy. *Toxicol Sci* **149**, 15–30 (2016).
- Li, A. S. & Marikawa, Y. An *in vitro* gastrulation model recapitulates the morphogenetic impact of pharmacological inhibitors of developmental signaling pathways. *Mol Reprod Dev* **82**, 1015–36 (2015).
- Augustine-Rauch, K., Zhang, C. X. & Panzica-Kelly, J. M. A developmental toxicology assay platform for screening teratogenic liability of pharmaceutical compounds. *Birth Defects Res B Dev Reprod Toxicol* **107**, 4–20 (2016).
- Marx-Stoelting, P. *et al.* A review of the implementation of the embryonic stem cell test (EST). The report and recommendations of an ECVAM/ReProTect Workshop. *Altern Lab Anim* **37**, 313–28 (2009).
- Arnold, S. J. & Robertson, E. J. Making a commitment: cell lineage allocation and axis patterning in the early mouse embryo. *Nat. Rev. Mol. Cell Biol.* **10**, 91–103 (2009).
- Bénazéraf, B. & Pourquié, O. Formation and segmentation of the vertebrate body axis. *Annu. Rev. Cell Dev. Biol.* **29**, 1–26 (2013).

31. Harbison, R. D. & Becker, B. A. Comparative embryotoxicity of diphenylhydantoin and some of its metabolites in mice. *Teratology* **10**, 237–241 (1974).
32. Matalon, S., Schechtman, S., Goldzweig, G. & Ornoy, A. The teratogenic effect of carbamazepine: a meta-analysis of 1255 exposures. *Reprod Toxicol* **16**, 9–17 (2002).
33. Brent, R. L. & Holmes, L. B. Clinical and basic science lessons from the thalidomide tragedy: what have we learned about the causes of limb defects? *Teratology* **38**, 241–251 (1988).

Acknowledgements

This work is supported by the Institute of Bioengineering and Nanotechnology, Biomedical Research Council, A*STAR; and Exploit Technologies Pte Ltd, A*STAR (ETPL/14-R15GAP-0006).

Author Contributions

J.X. and H.Y. designed the experiment. J.X., Y.C., H.L. and Z.S. did the data acquisition. J.X., Y.Y. and H.Y. analyze the data. J.X. and H.Y. wrote the manuscript.

Additional Information

Supplementary information accompanies this paper at doi:[10.1038/s41598-017-09178-1](https://doi.org/10.1038/s41598-017-09178-1)

Competing Interests: The authors declare that they have no competing interests.

Publisher's note: Springer Nature remains neutral with regard to jurisdictional claims in published maps and institutional affiliations.



Open Access This article is licensed under a Creative Commons Attribution 4.0 International License, which permits use, sharing, adaptation, distribution and reproduction in any medium or format, as long as you give appropriate credit to the original author(s) and the source, provide a link to the Creative Commons license, and indicate if changes were made. The images or other third party material in this article are included in the article's Creative Commons license, unless indicated otherwise in a credit line to the material. If material is not included in the article's Creative Commons license and your intended use is not permitted by statutory regulation or exceeds the permitted use, you will need to obtain permission directly from the copyright holder. To view a copy of this license, visit <http://creativecommons.org/licenses/by/4.0/>.

© The Author(s) 2017